Optics Letters

Optical transmission of a moving Fabry–Perot interferometer

Nazar Pyvovar and Lingze Duan*

Department of Physics and Astronomy, The University of Alabama in Huntsville, Huntsville, AL 35899, USA
**lingze.duan@uah.edu*

Received 11 September 2023; revised 25 October 2023; accepted 6 December 2023; posted 6 December 2023; published 8 January 2024

Fabry–Perot interferometers have been widely studied and used for well over a century. However, they have always been treated as stationary devices in the past. In this Letter, we investigate the optical transmission of a longitudinally moving Fabry–Perot interferometer within the framework of relativity and establish a general relation between the transmission coefficient and the velocity for uniform motions. Several features of the transmission spectrum are analyzed, with special attentions given to the non-relativistic regime, where application prospects are evaluated. New, to the best of our knowledge, potential interferometric schemes, such as velocity-scanning interferometry and hybrid interferometers based on nested configurations, are proposed. Finally, a special case of non-uniform motion is also investigated.

https://doi.org/10.1364/OL.505622

Introduction. The Fabry–Perot interferometer (FPI) is one of the most well-known optical instruments and has been widely used in many fields of science and technology [1,2]. In recent years, the advances in hybrid interferometers have created a new modality of utilizing the FPI. These hybrid schemes typically involve nesting the FPI in a "host" interferometer, such as a Michelson interferometer [3–5] or a Mach–Zehnder interferometer [6]. When the FPI operates under the resonance condition, it folds a long optical path inside and hence extends the effective arm length of the host interferometer, which often leads to much improved phase sensitivities. Such schemes have found tremendous success in gravitational wave detection [7] and have achieved record-setting strain resolutions in fiber-optic sensing [6].

Making the FPI a part of another interferometer also provokes an interesting thought: what if the FPI is moving relative to the host interferometer? The question stems from an intuitive rationale: since the FPI is intimately linked to the optical path length in a nested interferometer, any potential phase change induced by a longitudinal motion of the FPI could result in a detectable signal at the output of the host interferometer. Answering this question necessitates a thorough understanding of the transmission properties of an FPI in relative motion with respect to its interrogation system, which usually includes the light source and the detector. Surprisingly, despite being extensively studied for over a hundred years [8], the FPI has always been treated as a "stationary"device. This may sound erroneous at first, because, after all, one of the most common ways of using the FPI is by scanning its mirrors [9]. However, there is a fundamental distinction between a conventional "scanning"FPI and a "moving"FPI to be discussed here, as illustrated in Fig. 1. In the former case, the length of the FPI is tuned by changing the position of one of the mirrors. Since position is inherently a stationary quantity, the scanning FPI still operates on the premise that the FPI remains stationary with respect to its interrogation system in the lab frame. In the latter case, however, the FPI under concern is rigid and moves as a unit. The relevant question becomes how the states of motion, such as velocity and acceleration, impact the optical properties of the FPI.

This Letter presents our study of motion-induced transmission properties for a moving FPI. Before analyzing specific cases, let us first define the general problem under investigation. Consider an FPI formed by two-plane mirrors facing each other, with an optical medium set in between. The FPI is situated on a moving stage, which travels along the optical axis as indicated in Fig. 1(b). A collimated beam of light propagating along the optical axis interrogates the FPI under normal incidence, and the transmitted light is monitored by a photodetector. Both the light source and the detector are located in the lab (rest) frame.

In the following, we will examine the transmission coefficient of the FPI under uniform motion and discuss how its velocity dependence affects the amplitude, frequency, and phase of the transmitted light. New interferometric schemes are proposed for velocity and acceleration measurements by means of a moving FPI. The theoretical framework is also generalized to certain cases of arbitrary motion.

Uniformly moving FPI. *General theory*. In the case of a stationary FPI, given an incident wave E_I, the transmitted wave E_T can be found by summing up all the transmitted wavefronts across many round trips, as illustrated in Fig. 2(a):

$$E_T = E_0 + E_1 + E_2 + \cdots . \tag{1}$$

Assuming the two mirrors of the FPI have the same transmission and reflection coefficients t and r, respectively, and taking into account the round-trip phase delay, it is easy to show that

$$E_T = E_I t^2 e^{-ikd} \sum_{N=0}^{\infty} r^{2N} e^{-2iN \cdot nkd}, \tag{2}$$

where n is the refractive index of the material that the FPI is composed of, k is the wave number in vacuum, and d is the

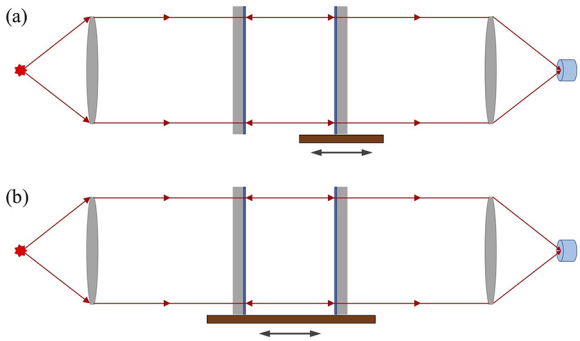

Fig. 1. Conceptual schemes of (a) a conventional scanning FPI and (b) a moving FPI.

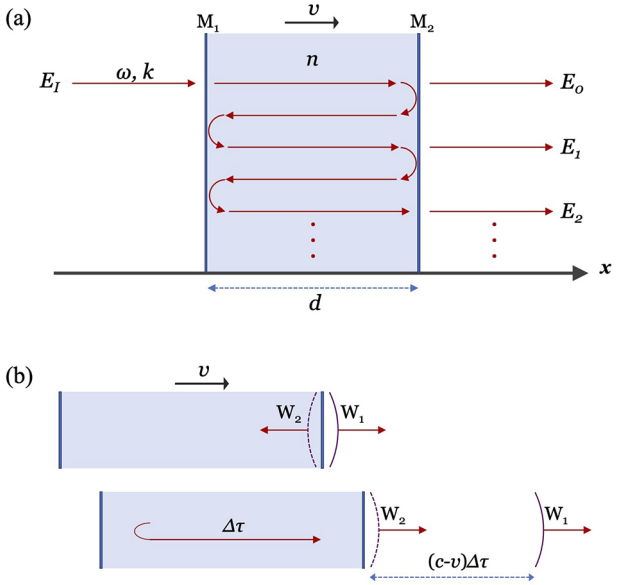

Fig. 2. (a) Concept of multiple wave superposition for a uniformly moving FPI. (b) Finding the round-trip phase delay by following the propagation of a wavefront.

length of the FPI. By defining the transmission coefficient of the FPI, $T \equiv E_T/E_I$, we have

$$T = \frac{t^2 e^{-inkd}}{1 - r^2 e^{-2inkd}}. \tag{3}$$

This derivation may be straightforwardly generalized to the case of a uniformly moving FPI, with the only change appearing in the phase of each wavefront E_N. Consider two successive wavefronts W_1 and W_2 as shown in Fig. 2(b). While W_2 completes a round trip inside the FPI, W_1 travels a distance $c\Delta\tau$, where $\Delta\tau$ is the round-trip time of the cavity. When W_2 finishes its trip inside the FPI and emerges from the mirror M_2, the FPI has already moved forward by a distance $v\Delta\tau$. Therefore, the phase difference between W_1 and W_2 is

$$\Delta\phi = k(c - v)\Delta\tau. \tag{4}$$

Meanwhile, it can be shown that the round-trip time inside the FPI is given by

$$\Delta\tau = \frac{d'}{(c/n_-) + v} + \frac{d'}{(c/n_+) - v}, \tag{5}$$

where d' is the length of the cavity measured in the lab frame and n_- and n_+ are the refractive indices experienced by the backward and forward traveling waves, respectively. Note that, due to the relativistic transformation of refractive index, the medium inside a moving FPI becomes anisotropic. This effect is called Fizeau's light-dragging effect [10–12]. The n_+ and n_- can be found by [13,14]

$$n_\pm = \frac{n \pm \beta}{1 \pm n\beta}, \tag{6}$$

where $\beta = v/c$. Notice further that, due to relativistic length contraction, $d' = d/\gamma$, where $\gamma = 1/\sqrt{1 - \beta^2}$. Substituting n_+, n_- and d' into Eq. (5) yields

$$\Delta\tau = \frac{2nd}{c}\gamma. \tag{7}$$

The phase delay between consecutive wavefronts is given by

$$\Delta\phi = 2nkd\sqrt{\frac{1 - \beta}{1 + \beta}}. \tag{8}$$

This round-trip phase shift is used to replace $\Delta\phi = 2nkd$ in Eq. (3), and the transmission coefficient for a uniformly moving FPI can be written as

$$T = \frac{t^2 e^{-i\zeta nkd}}{1 - r^2 e^{-2i\zeta nkd}}, \tag{9}$$

where ζ is defined as

$$\zeta = \sqrt{\frac{1 - \beta}{1 + \beta}}. \tag{10}$$

Comparing Eq. (9) with Eq. (3), it is evident that the impact of the uniform motion on the transmission property of the FPI is to introduce a velocity-dependent scaling factor $\zeta(v)$ in the round-trip phase. In fact, it can be shown that ζ simply represents a relativistic Doppler shift [15] associated with frame changes.

Frequency rescaling. The scaling factor $\zeta(v)$ causes some interesting changes to the transmission spectrum of a moving FPI. This becomes clear when we examine the transmittance of the FPI, which takes the form of the well-known Airy function, with an added velocity dependence:

$$|T|^2 = \frac{1}{1 + (4\mathcal{F}^2/\pi^2)\sin^2(\zeta(v)nkd)}, \tag{11}$$

where $\mathcal{F} \equiv \pi r/(1 - r^2)$ is the finesse of the FPI. Clearly, this is a generalization of the FPI transmittance for a stationary cavity, which now becomes a special case of Eq. (11) with $\zeta(v) = 1$ ($v = 0$). The resonance condition of the FPI is now given by $\zeta(v)nkd = m\pi$, where m is an integer representing the index of the resonance mode. The condition can be rewritten in terms of wavelength as $m\lambda = 2\zeta(v)nd$ or in terms of optical frequency as $\nu_m = m/[\zeta(v)\Delta\tau_0]$, where ν_m is the frequency of the mth mode and $\Delta\tau_0 = 2nd/c$ is the cavity round-trip time at rest.

In almost all practical cases, the FPI operates in the nonrelativistic limit, where $\beta \ll 1$. Under this condition, the resonance frequencies are given by

$$\nu_m = \frac{m}{\Delta\tau_0}\left(1 + \frac{v}{c}\right). \tag{12}$$

This resonance condition is similar to that of a stationary FPI except for the extra scaling factor $1 + v/c$. With a positive velocity, i.e., when the FPI travels in the same direction as the incident

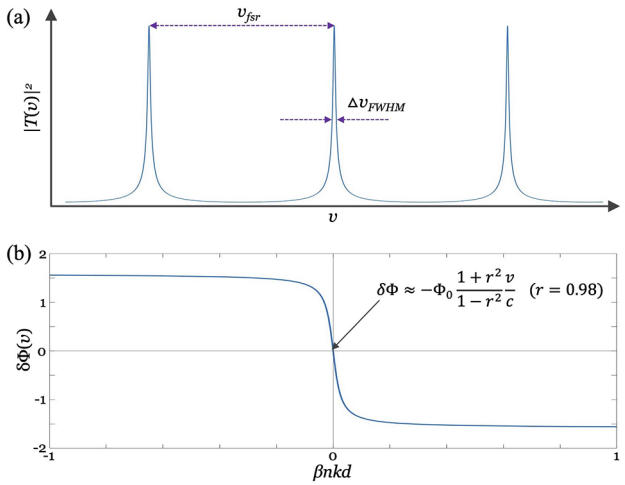

Fig. 3. (a) Transmittance of a velocity-scanning FPI has periodic transmission peaks against velocity v. FSR and FWHM can be defined accordingly. (b) The transmission phase has a near linear velocity dependence when $|\beta nkd|$ is small.

light, this scaling factor is greater than 1, which means the mode spacing grows larger than a stationary FPI. The actual frequency shift for the mth mode is $mv/(\Delta\tau_0 c)$. Such a frequency shift can be well within the detectable range even for small velocities, e.g., 1 cm/s. This is because the index m for a typical-sized FPI operating at an optical wavelength is very large (10^6–10^7).

It is also interesting to point out that the motion of the FPI also causes a rescaling of the transmission linewidth of the FPI by the factor $\zeta(v)$. For example, a positive nonrelativistic velocity would broaden the transmission line by a factor $1 + v/c$.

Velocity-scanning FPI. Meanwhile, the velocity dependence of FPI transmission leads to a new way to operate the FPI: scanning its longitudinal velocity. In the nonrelativistic regime, the transmittance of a moving FPI can be written as

$$|T(v)|^2 = \frac{1}{1 + (2\mathcal{F}/\pi)^2 \sin^2[nkd(1 - v/c)]}. \tag{13}$$

$|T(v)|^2$ is a periodic function of v, as illustrated in Fig. 3(a). Such a relationship is analogous to that of a scanning FPI, where $|T(d)|^2$ is a periodic function of the cavity length d. The resonance peaks appear when the velocity satisfies the condition $v/c = 1 - m(\lambda/2nd)$, where $\lambda \equiv 2\pi/k$ is the wavelength. A free spectral range (FSR) v_{fsr} can be defined as the spacing between adjacent resonance peaks, and v_{fsr} is given by

$$v_{fsr} = \frac{\lambda}{2nd}c = \frac{\lambda}{\Delta\tau_0}. \tag{14}$$

The linewidth of the resonance peaks is characterized by their full-width at half-maximum (FWHM) Δv_{FWHM}, which is given by

$$\Delta v_{FWHM} = \frac{\lambda}{\Delta\tau_0}\frac{1 - r^2}{\pi r} = \frac{v_{fsr}}{\mathcal{F}}. \tag{15}$$

To put the above analysis in a practical context, a 1 m glass ($n = 1.5$) FPI interrogated by a laser of $\lambda = 600$ nm would have a FSR $v_{fsr} = 60$ m/s. If the FPI has a finesse $\mathcal{F} = 1000$, the characteristic width of the resonance peaks is $\Delta v_{FWHM} = 6$ cm/s, which gives the velocity resolution of the FPI as a velocity discriminator. Such velocity discriminators offer a complementary approach to existing FPI-based velocimetry schemes, which typically rely on either scanning FPI discriminators [16] or stationary FPI discriminators [17].

Velocity discriminator. The concept of using a moving FPI as a velocity discriminator can also be investigated from the perspective of transmission phase. In general, the transmission coefficient of an FPI can be written as $T = |T| \exp(-i\Phi)$, where Φ is the transmission phase. From Eq. (9), it is easy to show that Φ is given by

$$\Phi = \zeta nkd + \arctan\left(\frac{r^2 \sin(2\zeta nkd)}{1 - r^2\cos(2\zeta nkd)}\right), \tag{16}$$

or equivalently

$$\tan\Phi = \frac{1 + r^2}{1 - r^2}\tan(\zeta nkd). \tag{17}$$

Taking $\zeta \approx 1 - \beta$ for nonrelativistic motion and using the resonance condition that requires nkd to be an integer multiple of π, the transmission phase can be rewritten as $\Phi = \Phi_0 + \delta\Phi(v)$, where $\Phi_0 = nkd$ is the steady-state transmission phase when the FPI is stationary. $\delta\Phi(v)$ is a small velocity-dependent phase change caused by the motion and is given by

$$\delta\Phi(v) = -\beta nkd - \arctan\left(\frac{r^2 \sin(2\beta nkd)}{1 - r^2\cos(2\beta nkd)}\right). \tag{18}$$

In Fig. 3(b), $\delta\Phi(v)$ is plotted against βnkd with both positive and negative velocities. Apparently, when $|\beta nkd|$ is small, $\delta\Phi(v)$ has a linear dependence over v. This linear relation can be found by taking the first-order approximation of Eq. (18), which yields

$$\delta\Phi(v) \approx -\Phi_0\frac{1 + r^2}{1 - r^2}\frac{v}{c}. \tag{19}$$

We are now ready to revisit the question raised at the beginning of the Letter: in a hybrid interferometer, where an FPI is used to fold the optical path, what would happen if the FPI begins to move? When an FPI operating in resonance begins to move longitudinally, albeit "slowly", the transmitted light experiences a small phase shift given by Eq. (19). The "−"sign indicates that, when the FPI moves toward the same direction as the optical wave, the phase change is negative. The amount of this phase shift is proportional to the steady-state transmission phase Φ_0, the velocity v, as well as the factor $(1 + r^2)/(1 - r^2)$. Clearly, long cavity length (large Φ_0) and high finesse ($r \to 1$) leads to high velocity sensitivity of $\delta\Phi(v)$.

It should be noted that the approximation Eq. (19) is only valid when $2\beta nkd \ll 1$, or in other words, $v \ll c/2nkd$. To put this condition in context, for a 1-cm-thick glass etalon operating at a wavelength of 600 nm, $c/2nkd \approx 1$ km/s, i.e., about three times the speed of sound in the air. Therefore, for cavities of common sizes, Eq. (19) remains valid for most practical cases.

Hybrid interferometers. The velocity sensitivity of the transmission phase enables highly sensitive velocity measurement using hybrid interferometer configurations. Two possible schemes are shown in Fig. 4, and more variations can potentially be conceived. In the first scheme [Fig. 4(a)], a balanced Mach–Zehnder interferometer (MZI) is used as the host interferometer, with two identical FPIs serving as optical path multipliers. Such a hybrid configuration has been experimentally demonstrated in fiber-optic systems [6]. Now, if one of the FPIs begins to move longitudinally while the other remains stationary, an extra phase difference is generated between the two

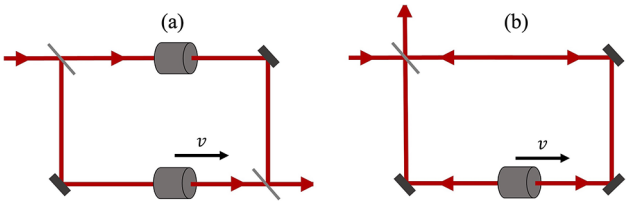

Fig. 4. Examples of hybrid interferometers with a moving FPI incorporated: (a) balanced Mach–Zehnder interferometer and (b) Sagnac interferometer.

arms according to Eq. (19), causing a detectable signal at the output of the MZI.

In the second scheme, a single FPI is integrated into a Sagnac interferometer (SI), as shown in Fig. 4(b). Under the steady state with the FPI at rest, the clockwise and the counterclockwise circulating beams experience the same optical path inside the FPI. When the FPI moves toward one direction, however, this symmetry between the two directions is broken, and a phase shift $\delta\Phi_{SI}$ is created between the two beams at the output port of the SI. Note that the velocity sensitivity of the SI configuration is twice as large as the MZI configuration:

$$\delta\Phi_{SI} = 2\Phi_0 \frac{1+r^2}{1-r^2}\frac{v}{c}. \tag{20}$$

Therefore, for velocity and acceleration measurements using moving FPIs, the simpler SI configuration may be a more preferable scheme.

Adiabatic non-uniform motion. The above theory for a uniformly moving FPI can be easily generalized to describe the adiabatic non-uniform motion (ANUM). Here, the term "adiabatic"refers to the condition where the change of velocity is so "slow"that, at any moment of time, the FPI can be approximately treated as being in a state of uniform motion. Physically, this requires the change of velocity during the effective "storage time"of the FPI to be less than what the FPI can discriminate. Analytically, we can describe this condition simply as $(dv/dt)\tau_{cav} < \Delta v_{FWHM}$, where τ_{cav} is the cavity storage time for an FPI and is typically given by $\tau_{cav} = 2nd\mathcal{F}/(\pi c)$ [18]. Using Eq. (15), the ANUM condition can be written as

$$a < \frac{\pi\lambda}{\Delta\tau_0^2\mathcal{F}^2}, \tag{21}$$

where $a \equiv dv/dt$ is acceleration. Again, let us put this relation into context by applying the following typical values: $d = 0.1$ m, $n = 1$, $\mathcal{F} = 1000$, and $\lambda = 600$ nm. The corresponding ANUM condition is $a < 4 \times 10^6$ m/s^2, which is about 4×10^5 times the Earth's gravity acceleration. Therefore, for most foreseeable applications, the ANUM condition should be well satisfied.

Under the ANUM condition, the transmission coefficient of the FPI adiabatically follows the change of the velocity such that

$$T(\tau) = \frac{t^2 e^{-i\zeta(\tau)nkd}}{1 - r^2 e^{-2i\zeta(\tau)nkd}}, \tag{22}$$

where $\zeta(\tau)$ is defined as

$$\zeta(\tau) = \sqrt{\frac{1 - v(\tau)/c}{1 + v(\tau)/c}}. \tag{23}$$

Conclusion. In conclusion, we have analyzed the transmission coefficient of a uniformly moving FPI and have shown the impact of velocity on the frequency rescaling. A close look at the transmittance of the FPI has led to the definitions of FSR and FWHM on the scale of velocity as well as the new concept of velocity-scanning Fabry–Perot. Meanwhile, the transmission phase of the FPI is shown to feature a sharp linear slope around the resonance velocities, which allows a moving FPI to be used directly for velocity and acceleration measurements. As examples, hybrid interferometric schemes based on nested MZI-FP and SI-FP configurations are proposed. We hope that this work can offer a new perspective to the century-old device FPI.

Funding. National Science Foundation (ECCS-1606836).

Disclosures. The authors declare no conflicts of interest.

Data availability. No data were generated or analyzed in the presented research.

REFERENCES

1. G. Hernandez, *Fabry–Perot Interferometers, Cambridge Studies in Modern Optics*, 3rd ed. (Cambridge University Press, 1988).
2. J. M. Vaughan, *The Fabry–Perot Inteferometer: History, Theory, Practice and Applications*, 1st ed. (Routledge, 1989).
3. B. P. Abbott, Rep. Prog. Phys. **72**, 076901 (2009).
4. C. Gräf, S. Hild, H. Lück, *et al.*, Classical Quantum Gravity **29**, 075003 (2012).
5. T. A. Al-Saeed and D. A. Khalil, Optik **242**, 167170 (2021).
6. N. M. R. Hoque and L. Duan, Sci. Rep. **12**, 12130 (2022).
7. R. Weiss, Rev. Mod. Phys. **90**, 040501 (2018).
8. C. Fabry and A. Perot, Ann. de Chim. et de Phys. **16**, 115 (1899).
9. J. V. Ramsay, Appl. Opt. **1**, 411 (1962).
10. H. Fizeau, Comptes Rend. Acad. Sci. **33**, 349 (1851).
11. H. A. Lorentz, Proc. K. Ned. Akad. Wet. **6**, 809831 (1904).
12. P. C. Kuan, C. Huang, W. S. Chan, *et al.*, Nat. Commun. **7**, 13030 (2016).
13. W. Chyla, Optik **124**, 1477 (2013).
14. The relativistic transformations for the optical constants of media.
15. S. Ataman, Eur. J. Phys. **42**, 025601 (2021).
16. A. Courteville, Y. Salvadé, and R. Dändliker, Appl. Opt. **39**, 1521 (2000).
17. C. F. McMillan, D. R. Goosman, N. L. Parker, *et al.*, Rev. Sci. Instrum. **59**, 1 (1988).
18. M. J. Lawrence, B. Willke, M. E. Husman, *et al.*, J. Opt. Soc. Am. B **16**, 523 (1999).